Haptogram: Ultrasonic Point-Cloud Tactile Stimulation

GEORGIOS KORRES, (Member, IEEE), AND MOHAMAD EID, (Senior Member, IEEE)
New York University Abu Dhabi, Abu Dhabi 129188, United Arab Emirates

Corresponding author: M. Eid (mohamad.eid@nyu.edu)

ABSTRACT Studies of the stimulating effect of ultrasound as a tactile display have recently become more intensive in the haptic domain. In this paper, we present the design, development, and evaluation of Haptogram; a system designed to provide point-cloud tactile display via acoustic radiation pressure. A tiled 2-D array of ultrasound transducers is used to produce a focal point that is animated to produce arbitrary 2-D and 3-D tactile shapes. The switching speed is very high, so that humans feel the distributed points simultaneously. The Haptogram system comprises a software component and a hardware component. The software component enables users to author and/or select a tactile object, create a point-cloud representation, and generate a sequence of focal points to drive the hardware. The hardware component comprises a tiled 2-D array of ultrasound transducers, each driven by an FPGA. A quantitative analysis is conducted to measure the Haptogram ability to display various tactile shapes, including a single point, 2-D shapes (a straight line and a circle) and a 3-D object (a hemisphere). Results show that all displayed tactile objects are perceivable by the human skin (an average of 2.65 kPa for 200 focal points). A usability study is also conducted to evaluate the ability of humans to recognize 2-D shapes. Results show that the recognition rate was well above the chance level (average of 59.44% and standard deviation of 12.75%) while the recognition time averaged 13.87 s (standard deviation of 3.92 s).

INDEX TERMS Haptic interfaces, human computer interaction, ultrasonic transducer array, user interfaces.

I. INTRODUCTION

Recently, interest in 3D interaction has grown exponentially. A major drive for this tendency is the widespread of 3D content generation, authoring, and display interfaces (such as 3D scanners, printers, visual display interfaces, and hologram technologies). Adding haptic feedback to these interfaces enables users to experience the physical properties of interaction objects such as the stiffness, texture, and mass.

A haptic interface renders touch sensations at the human skin through either tactile or kinesthetic feedback. Haptic interfaces have been commonly used in a wide spectrum of applications, including virtual reality, tele-operation, interpersonal communication, entertainment and gaming, military, and health care [1]. A fascinating method for tactile stimulation is to use mid-air stimulation technologies (also known as contactless tactile interfaces) [2]. Mid-air stimulation seeks transmitting tactile stimulus without any physical contact between the haptic device and the human body.

Existing technologies to provide mid-air tactile stimulation use three strategies: (1) Air-Jet [3], [4], (2) ultrasound [2], and (3) laser [5]. Air jets rely on air pulses generation directed by an actuated flexible nozzle to provide tactile sensation.

Although they are effective in simulating rough force feedback, Sodhi et al. demonstrated air-jet tactile display up to 1 m distance with a resolution of 8.5 cm [3], their spatial/temporal properties are limited. Laser can travel longer distance with little diffusion and attenuation and thus could create a larger workspace of tactile display, however it requires a light-absorbing elastic medium attached to the skin. Ultrasonic tactile stimulation seems the most studied approach due to its ability to generate relatively high-resolution tactile displays in 3D space.

Ultrasonic tactile stimulation involves focusing multiple ultrasound beams in one or more focal points to produce tangible mid-air acoustic pressure effect [6]. When a transducer array is driven such that the phases of the ultrasonic waves coincide at a point (called the focal point), the radiation pressure will be strong enough to be perceivable by human skin. In this paper we introduce Haptogram, a novel system that renders point-cloud 3D tactile objects. Haptogram produces 3D tactile sensation by animating focal points at high speed so humans feel the distributed points simultaneously. We describe the Haptogram system and present a performance analysis study to characterize the Haptogram system

as a haptic interface. Finally, we conduct a usability study with 2D tactile objects to evaluate the user experience.
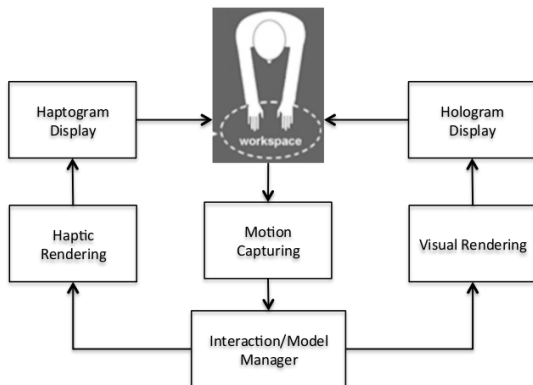

FIGURE 1. Immersive haptic-visual system.

The ultimate goal of the Haptogram system is to create a touchable hologram as shown in Figure 1. Visual rendering generates the graphics to be displayed by the hologram display where the haptic rendering calculates the tactile forces that must be displayed by the Haptogram system. The remainder of the paper is organized as follows: Section II presents the related work. Section III presents the modeling of the ultrasound-based tactile display, and the hardware/software design. In section IV, we present a study to characterize the Haptogram system as a haptic interface for displaying 2D/3D tactile shapes, including an experimental setup, procedure, and results. Section V presents a usability study with four 2D shapes. Finally, section VI summarizes the paper and provides perspectives for future work.

II. RELATED WORK
Ultrasonic tactile stimulation relies on acoustic waves that are focused on the human skin to produce compressed air [7]. Early studies by Dalecki et al. demonstrated that tactile sensations can be evoked from the ultrasound radiated on the skin in the water [2]. A subsequent work by Shinoda and colleagues used a 2D array of ultrasonic transducers to produce spatio-temporal stress patterns on a 2D plane of 1 by 1 cm area [8]. Results showed that octagonal arrangement of the array could produce a well-focused force spot to be animated in the display area. Since then, there has been a significant progress in this area to investigate ultrasound tactile display.

Shinoda and colleagues have made significant contributions with airborne ultrasound tactile stimulation to enhance the quality of the tactile display (workspace, intensity, and rendering) and integrate it with mid-air visual display. A feasibility study with 91 transducers was conducted to generate a fixed focal point [9]. A subsequent work introduced a tactile display, consisting of 324 transducers, to add movement of the focal point and produce tangible forces of around 16 mN (20 mm spatial resolution and 1 kHz vibrations) [10]. Experiments showed that users were able to discriminate tactile stimulation moving direction. This tactile display was

then improved, with 2,241 transducers, to offer a much larger workspace (1 m^3) and an improved temporal resolution of 0.5 ms [11]. The system was then integrated with visual feedback to enable noncontact blind touch interaction by adding tactile feedback variation for notifying the finger location [12], [13]. The latest development by Shinoda's team was to produce a 3D spatially standing haptic image via ultrasonic stimulation that does not require hand tracking [14]. Compared to the previous work, the proposed method does not require any temporal ultrasonic modulation and thus the tactile display is completely silent.

Gavrilov proposed a method to display 2D tactile shapes by generating multiple focal points [15]. This method was extended into UltraHaptics; a multi-point tactile feedback system used over an interactive visual screen. UltraHaptics is capable of producing independent tactile stimulation points, by utilizing temporal multiplexing, in relation to on-screen elements, within a target range of 20 cm [16]. A subsequent work involved displaying 3D volumetric haptic shapes in mid-air [17]. An algorithm for controlling the volumetric distribution of the sound pressure field in the form of 3D shape is proposed and evaluated. A similar endeavor for rendering volumetric tactile shapes via ultrasound is demonstrated in [18]. The characteristics of the ultrasonic pressure field created by ultrasonic transducers are also a relevant field of research (such as output force, number of transducers, frequency, spatial resolution and workspace, and power consumption. In [19], an approach is presented for measuring the strength of the ultrasonic pressure field. The proposed system produced 1.6 gf (15.7 kPa) within the focal region and achieved a spatial resolution of 20 mm. Furthermore, [20] explored the overall radiation pressure field of a system comprising of two ultrasonic transducers with different radiation frequencies. Simulation results closely agreed with experimental measurements and the paper concluded with considerations for designing dual-frequency ultrasound systems. Hoshi proposed an aerial-input aerial-tactile-output system that utilizes a Kinect device and ultrasound to produce tactile feedback in mid-air [21]. The tactile display system is composed of a PC, a master-slave system and two ultrasound arrays of 96 transducers each. The target workspace is $200 \times 200 \times 200$ mm, and is divided into $5 \times 5 \times 12.5$ mm sub-areas. Each of these sub-areas can be a target focal point that stimulates tactile feedback in mid-air.

In summary, existing work for displaying tactile objects utilizes volumetric or point-based stimulation. Volumetric stimulation is limited by its ability to display complex 3D tactile objects, whereas point-based stimulation is limited to rendering one or few points of tactile rendering. In this paper, we present a point-cloud approach for rendering 2D/3D tactile shapes using a discrete number of focal points without the need for a hand tracker (since a perceptual 3D tactile object is floating in 3D space). The phase information corresponding for generating all these focal points are computed and stored in a hardware controller. Displaying a 3D tactile object involves switching from one focal point to the next

at an extremely high speed since the phase information is all stored in the hardware controller. Two experiments are presented to validate the approach: experiment 1 to evaluate the performance of Haptogram to display various 2D/3D tactile objects, and experiment 2 to evaluate the usability with 2D tactile shapes.
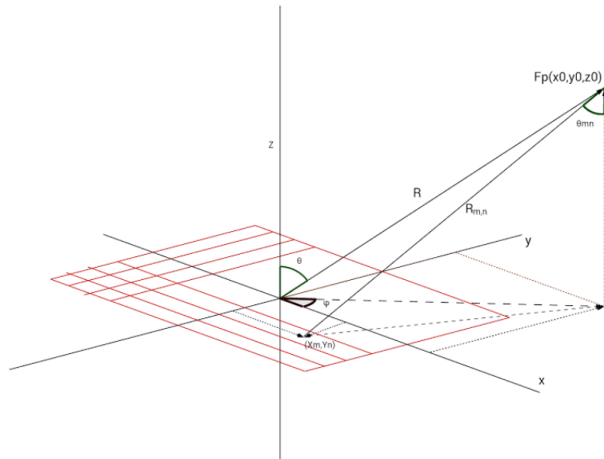

FIGURE 2. Coordinate system.

III. HAPTOGRAM SYSTEM
A. ACOUSTIC PRINCIPLES AND MODELING
Consider the coordinate system shown in Figure 2, with a 2D ultrasound array of MxN transducers and an arbitrary focal point F_p shown in equation (1). The distance between the focal point and each transducer is divided by the speed of sound to find the ultrasound wave travel time t_{mn} for each transducer as shown in equation (2) —so that the ultrasound waves come in phase at the focal point to generate acoustic pressure. In equation (1), R is the distance from the origin to the focal point, θ is the incident angle, and ϕ is the rotational angle. The focal law can be obtained from equation (3), and thus the transducers delays are calculated via equation (5), as shown in [22].

$$F_p = (R \sin\theta \cos\phi, R \sin\theta \sin\phi, R \cos\theta) \qquad (1)$$

Then for any transducer E_{mn} at $(x_m, y_n, 0)$:

$$t_{mn} = \frac{\|F_p - E_{mn}\|}{c} \qquad (2)$$

$$\tau_{mn} = \max(t_{mn}) - t_{mn} \qquad (3)$$

$$\Delta T = \max(t_{mn}) - \min(t_{mn}) \qquad (4)$$

$$\Delta\tau_{mn} = [\tau_{mn}] \bmod \left[\frac{\lambda}{c}\right] \qquad (5)$$

Where [] denote the integer part in equation (5), λ the wavelength, c the sound speed, and $\Delta\tau_{mn}$ is the time shift per transducer in order for all of them be in phase at the focal point. The pressure from a transducer E_{mn}, assuming a point source modeling, can be described as an outgoing spherical wave using equation (6), where A is the maximum pressure,

R is the distance from the transducer to the focal point, ω is the angular frequency, t is the time, and k is the wave number.

$$p(R, t) = \frac{A}{R} e^{j(\omega t - kR)} \qquad (6)$$

For an array of transducers M*N, the pressure contributed by each transducer $p_{mn}(R_{mn}, t_{mn})$ is calculated as shown in equation (7), where $m, n = 1...M, N$. Note that R_{mn} is the distance between transducer E_{mn} and the focal point whereas t_{mn} is the time it takes the ultrasound wave to travel from transducer E_{mn} to the focal point.

$$p_{mn}(R_{mn}, t_{mn}) = \frac{A}{R_{mn}} e^{j(\omega t_{mn} - kR_{mn})} \qquad (7)$$

Where $R_{mn} = \sqrt{(x_0 - x_m)^2 + (y_0 - y_m)^2 + z_0^2}$ The total pressure can be derived as the superposition of the pressure generated by each transducer at the focal point $F_p = (x_0, y_0, z_0)$ by using the focal law [22]. The resulting formula for the pressure field is given by equation (8).

$$p(R, \theta, t) = \sum_{mn}^{MN} \frac{A}{R_{mn}} e^{j(\omega(t + \Delta T + \Delta\tau_{mn}) - kR_{mn})} \qquad (8)$$

A more precise modeling is to represent the transducer by a circular surface rather than a point source. Therefore, the transducer E_{mn} can be replaced by the far field approximation of the Rayleigh-Sommerfeld integral model [23] with a circular surface (piston) of radius α as shown in equation (9).

$$p_0(R, \theta, t) = j\omega\rho U_0 \alpha^2 . \sum_{mn}^{MN} \frac{e^{j(\omega(t + \Delta T + \Delta\tau_{mn}) - kR_{mn})}}{R_{mn}}$$
$$\times \left[\frac{J_1(k\alpha \sin\theta_{mn})}{k\alpha \sin\theta_{mn}} \right] \qquad (9)$$

Where $\theta_{mn} = \tan^{-1}\left(\frac{\sqrt{(x - x_m)^2 - (y - y_m)^2}}{z}\right)$ is the angle between R_{mn} and the axis perpendicular to transducers plane whereas J_1 is the first order Bessel function, U_0 is the uniform particle velocity generated by a circular surface of radius α, and ρ is the medium density. Note that the far field approximation is accurate for distances that satisfy the following condition:

$$R \gg \frac{d^2}{4\lambda}, \quad where \quad d = 2\alpha \qquad (10)$$

B. HAPTOGRAM SYSTEM OVERVIEW
The Haptogram system is composed of a software subsystem and a hardware subsystem (Figure 3). The software subsystem has three components: Graphical User Interface (GUI), 3D Point Cloud Representation (PCR) and Focal Point Calculation (FPC).

The GUI provides the end user with a standard interface to author tactile objects that can be displayed using the Haptogram system (single point, 2D or 3D objects). The user would author/select from a list of existing tactile objects and load the corresponding PCR into the FPGA memory for execution. A snapshot of the GUI is shown in Figure 4.
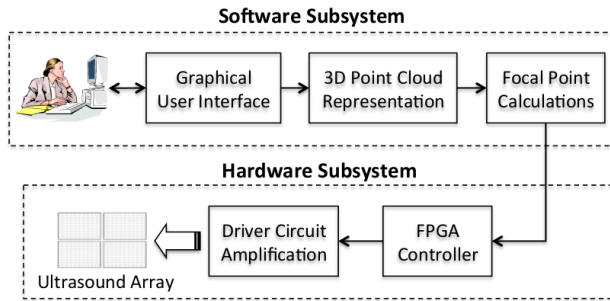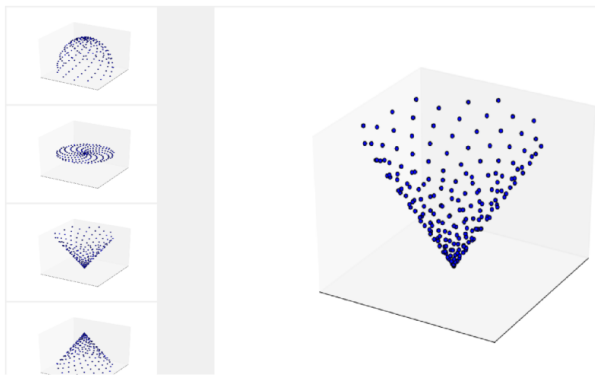
FIGURE 3. Overview of the Haptogram system.

FIGURE 4. Graphical User Interface for the Haptogram System, showing point cloud for various 3D tactile objects.

FIGURE 5. FPGA block diagram design.

FIGURE 6. Pulse generator output voltage waveform.

The PCR component calculates a finite set of points that approximate the authored shape. Each discrete point is represented by 3D coordinates (x,y,z) and is sent to the FPC component. The FPC component calculates the distances between each focal point and the transducers, and the timings/phases to produce the focal point. The FPC component stores the results in a hexadecimal file that is loaded into the FPGA Controller memory.

The hardware subsystem is made up of three components: the FPGA Controller, the Driver Circuit Amplification (DCA) component, and the Ultrasound Array (UA) consisted of V=100 ultrasound transducers. The FPGA Controller produces synchronized pulse signals that feed into the DCA. The DCA component is basically an amplifier circuit that produces sufficient power to actuate the ultrasound transducers. Finally, the UA is a composition of tiles of two-dimensional array of ultrasound transducers unit that are expandable to increase device workspace and intensity of tactile stimulation.

C. FPGA CONTROLLER DESIGN
The FPGA controller design, shown in Figure 5, consists of six basic sub-designs: The primary memory, the sequence memory, the UART serial port, the memory controller, the cycle controller, and the pulse generator.

Assuming a 3D object will be displayed via (V) number of focal points. All the information needed to form the (V) focal points is store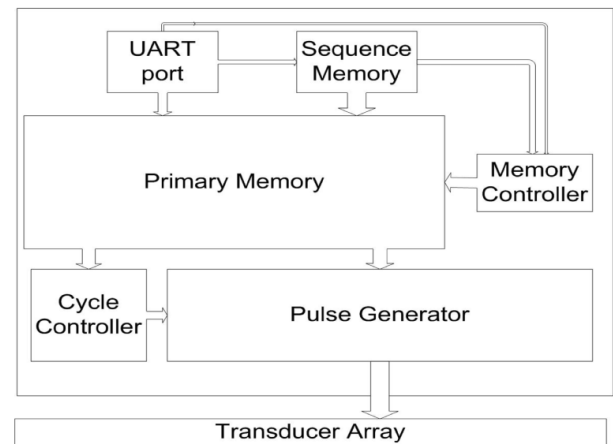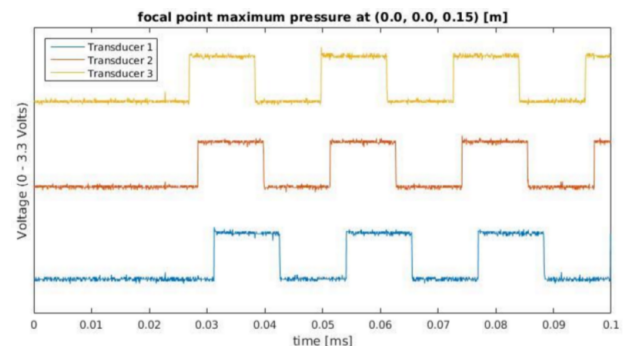d in the primary memory. The details of each focal point consist of: the timing queues for each transducer (100 16-bit numbers in total), the cycle length (period of the pulse, 24-bit), the pulse length (8-bit), and a pre-scalar clock divider (24-bit) value. The memory data is accessed via a script that is developed for this purpose (TCL script), through the JTAG interface.

In the sequence memory a series of index numbers between 1 and (V) is stored. The sequence memory drives the primary memory by using these indices to select the appropriate focal point to be formed at a specific time. The UART serial port drives the primary memory and enables/disables the sequence memory. Each time a focal point is to be changed, an index number is sent through the UART port. A specific index is used to activate or deactivate the sequence memory.

The memory controller extracts all the needed information out of the primary memory in order to form a single focal point. All the extracted data are loaded to the cycle controller and the pulse generator. The cycle controller determines the pulse duration and drives a 24-bit counter. The counter output is then fed to the pulse generator to produce the appropriate pulses. The cycle controller dictates the system to perform just once or repeat continuously.

The pulse generator is the most important sub-design of the FPGA. All the appropriate pulses are produced to create
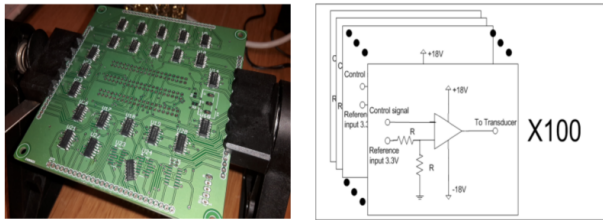
FIGURE 7. The ultrasound transducer amplification circuit.

the desired focal point. The data from the primary memory and from the cycle controller are fed to the pulse generator. The timing queue data provided by the primary memory is compared in each time step with the cycle controller value in such a way that the appropriate, separate, pulse for each transducer is generated at the appropriate time. Those pulses are finally fed to the transducer amplification circuit. An example of the voltage waveform for sample transducers is shown in Figure 6; note the phase shift between successive transducers to achieve acoustic pressure at the focal point.

D. THE AMPLIFICATION CIRCUIT

The FPGA controller produces the electric pulses needed to drive the transducer array to emit ultrasound waves. But before those pulses are fed to the array, they have to be driven through an amplification circuit that guarantees maximum power of the produced ultrasonic waves to achieve tangible tactile sensation. Each pulse is fed to the non-inverting input of an Op-Amp, which is configured as a voltage comparator, as shown in the circuit schematics of Figure 7. A reference voltage is fed to the inverting input of the Op-Amp. The maximum voltage supply of the Op-Amp is 20 Volts. The output of the amplification circuit is the same waveform except with 20 Volts rather than the 0-3.3 Volts generated by the FPGA. The output from each Op-Amp is then connected to the transducer array.
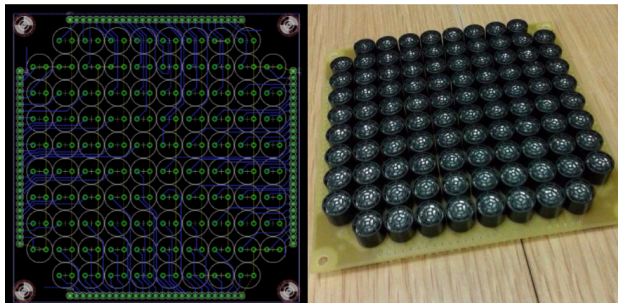

FIGURE 8. One tile design for the Haptogram display device.

E. THE ULTRASONIC ARRAY

The amplified signals are fed to a tiled two-dimensional array of ultrasound transducers. Each tile (shown in Figure 8) is a 10-by-10 array of ultrasound transducers that connects to the central FPGA. The MA40S4S 40 kHz Murata ultrasound transducer is used in the Haptogram system. Note that the more tiles the Haptogram system uses, the larger the tactile
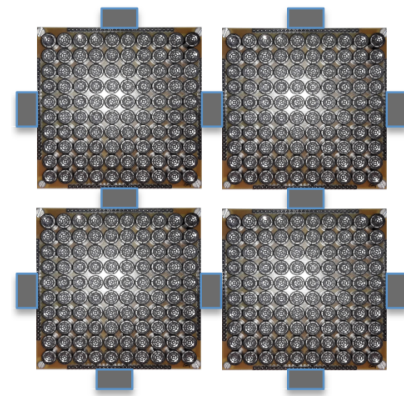

FIGURE 9. The Tiled two-dimensional array design.

display workspace is. Furthermore, the intensity of the tactile stimulation would increase as the number of display tiles increases.

The tiled two-dimensional array design, shown in Figure 9, has several advantages. First of all, a tiled display can be arbitrarily scaled to extend the 3D tactile stimulation workspace. Secondly, a tiled display provides a flexible display apparatus, increases tactile stimulation intensity, reduces manufacturing difficulties and provides substrate space for wiring and control circuits on the display tile substrate (thereby improving system integration).

F. FOCAL POINT CALCULATION

The focal point calculation occurs as follows. After importing the focal point coordinates (x,y,z), the distances and the timings between each transducer and the focal point are calculated. The timing data are used to calculate the phases for the control signals for the respective transducers. The process of calculating timings/phases is repeated for every focal point. The outcome is a list of timing data representing the focal points forming the 3D object. This final list is fed to a function that converts the list to an appropriate hex file using a modified version (for 16 and 32 bit words) of a library called intelhex. Finally, the hex file is loaded into the primary memory of the FPGA by calling a TCL script particularly designed for this purpose. A summary of the focal point calculation is depicted in the flowchart of Figure 10.

The TLC script is the interface between the software and the FPGA design. It drives the quartus_stp.exe that can edit the memory contents of the Altera FPGA via the JTAG programmer. It can also edit constants that are hardcoded in the FPGA fabric. The sequence memory contains a series of numbers (0 -V) and is responsible for driving the primary memory. For example if a user loads the sequence 1-2-3-4 fifty times (1-2-3-4-1-2-3-4 $\cdots$ 1-2-3-4) then the primary memory will form only the first four focal points for fifty times according in the same order.

G. TACTILE RENDERING

Given that the FPGA controller runs at a frequency f_P, the number of clock cycles needed to prepare te actuation signal
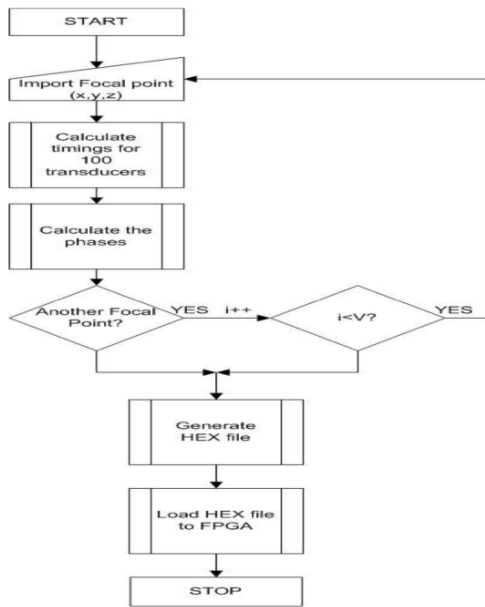
FIGURE 10. Focal point calculation flow chart.

for switching focal points is C, the frequency of ultrasound waves is f_U, then the time required to produce a focal point is $\frac{1}{f_U} + \frac{C}{f_P}$. However, additional time is needed for all transducers to contribute to the formation of the focal point to generate maximized pressure. The minimum number of pulses needed for all transducers to contribute to the formation of the focal point is denoted as β and is defined by equation (11), based on equation (4); note that β is an integer number. If the rendering frequency for the focal points is f_R , then the maximum number of focal points that can be generated to create a 2D/3D tactile object (V) is expressed in equation (13).

$$\beta = \left[f_U \left(\max \Delta t_{ij} - \min \Delta t_{ij} \right) \right] \qquad (11)$$

The total time needed to form maximized pressure at the focal point is given by equation (12).

$$T_f = \frac{\beta}{f_U} + \frac{C}{f_P} \qquad (12)$$

Where T_f is a critical for fast switching of focal points and is referred to as the Focal Point Formation (FPF) delay. This delay includes the time for the transducer to settle vibration amplitude since start of driving, dead time due to time of flight of the ultrasound wave, and propagation time.

Given V as the number of focal points, the rendering frequency f_R is defined as shown in equation (13).

$$V = \frac{\frac{1}{f_R}}{\frac{\beta}{f_U} + \frac{C}{f_P}} \qquad (13)$$

Equation (13) demonstrates an inversely proportional relationship between the rendering frequency and the number of focal points. This implies that generating higher resolution tactile display requires an increase in the number of focal points to form the tactile object. This in turn results in lower

rendering frequency (if maximum acoustic pressure per focal point is to be maintained where all transducers contribute to the focal point formation). On the other hand, in order to increase the rendering frequency of tactile objects, a decrease in the number of focal points (per object) is to be expected. It then becomes a user choice to pick the proper configurations of the Haptogram system to make specifications for a particular application.

In order to describe this relationship analytically, the current implementation of the Haptogram system utilizes a 10×10 array of ultrasonic transducers with a resonance frequency $f_u = 40\ kHz$, C = 108, and a processor clock $f_p = 50\ MHz$. Assuming that the center of the display workspace is at an elevation of 10 cm, equation (4) provides a calculation for $\Delta T = 643\ \mu s$. The minimum number of pulses for all transducers to contribute to the formation of a focal point is $\beta = 26$, based on equation (11). Therefore the relationship between the rendering frequency $V = \frac{10^3}{0.643 f_R}$. If a rendering frequency of 30 Hz is sufficient for a particular tactile display, then a total number of focal points of V = 51 can be achieved while maintaining maximized acoustic pressure. Note that a larger rendering frequency can still be achieved with the same number of focal points but with lower acoustic pressure. As long as humans perceive the generated acoustic pressure, such alterations remain valid system configurations.
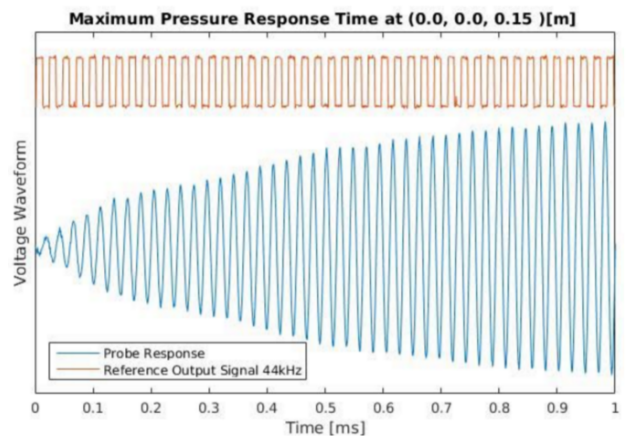

FIGURE 11. Focal point formation delay.

An experiment is conducted to measure the focal point formation delay using the current Haptogram prototype. An ultrasound receiver in used to measure the generated acoustic pressure at 15 cm elevation. Figure 11 shows the voltage waveform measured by the ultrasound receiver probing for the acoustic pressure at 15 cm elevation over time. Considering the 90% rise time, the FPF delay is measured to be around 640 μs, which seems consistent with the analytical result of 643 μs.

IV. PERFORMANCE EVALUATION
This section presents a performance study to demonstrate the effectiveness of point cloud tactile stimulation for

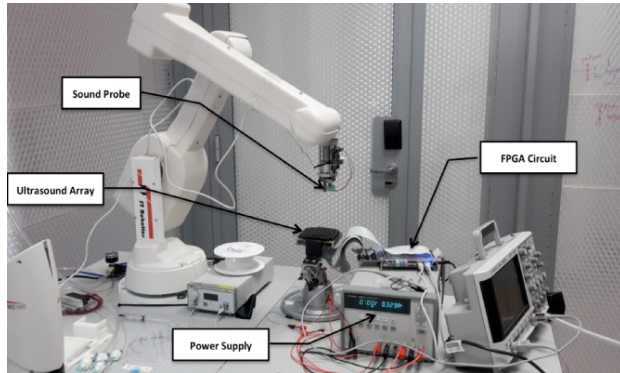single point, 2D shapes, and 3D shapes. The analysis is limited to one tile configuration.

FIGURE 12. The experimental setup.

FIGURE 13. Theoretical single-point stimulated at 13 cm elevation (scale in m).

FIGURE 14. Experimental single-point stimulated at 13 cm elevation (scale in mm).

A. EXPERIMENTAL SETUP

In order to measure the spatial distribution of the acoustic radiation pressure, we used the experimental setup shown in Figure 12. An ultrasonic sensor probe was attached to the end effector of the robotic arm (ST Robotics R17) whose resolution for movement is 0.1 mm.

The sound probe is an MA40S4R 40kHz Murata ultrasound transducer with a sensitivity of 0 dB (10 V/Pa). Its output was fed to an AC-to-DC conversion circuit (a rectifying bridge and then to an array of decoupling capacitors). Finally the resulting DC signal (which represents the sound intensity) is fed to a 10-bit analog to digital converter. The current was limited to 900 mA whereas the voltage was limited to 12 V. A simple script was developed to control the robotic arm to scan the workspace of the array to measure the distribution of sound pressure. Measurements are acquired every 1 mm around the focal point in the case of single point stimulation and 2 mm for 2D and 3D shapes. Twenty measurements are taken at every point with 1 ms intervals and the average is calculated as the force actuation at that position.

B. SINGLE POINT TACTILE STIMULATION

A single focal point is rendered at 1.852 kHz at the center of the array with an elevation of 13 cm (acoustic pressure flashing at 1.852 kHz at the focal point location). A cubical volume of $50 \times 50 \times 50$ mm centered at the focal point is scanned (step size of 1 mm along xy-plane thus giving a total of 2500 measurements for a single slice along the vertical axis, 10 slices along the z-axis are used with 5mm step size). We report only the pressure distribution at the desirable elevation.

Since the acoustic pressure amplitude turned out to be time varying, the average values are recorded. Figure 13 shows the theoretically calculated pressure distribution of the focal point at 13 cm elevation. Figure 14 shows the experimental distribution of the sound pressure around the focal point
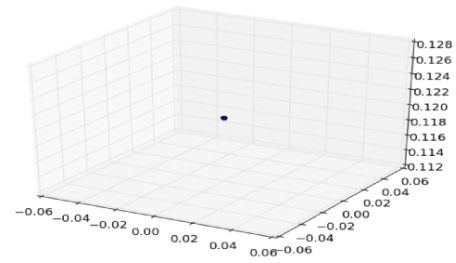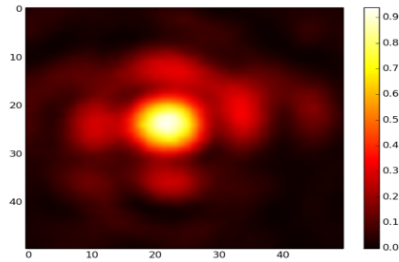
(at 13 cm elevation). The amplitude is normalized with a maximum acoustic pressure of 2.95 kPa. As shown in Figure 14, one focal point is clearly generated and its diameter is about 10 mm.
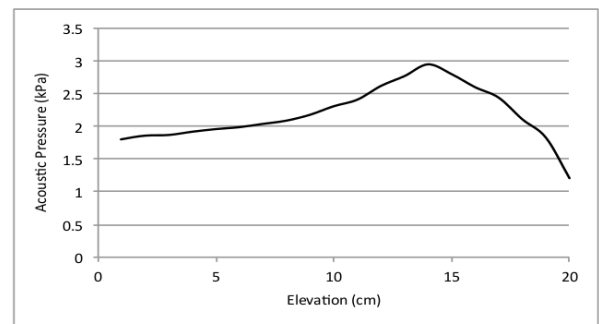

FIGURE 15. Forces versus distance for focal point stimulation.

Another study is conducted to estimate the elevation at which maximum acoustic pressure is generated for one tile configuration. We utilized a series of focal points starting from an elevation of 1 cm up to 20 cm and measured the corresponding acoustic pressure presented at each elevation, with a step size of 1 cm. The results, as shown in Figure 15, demonstrate that maximum acoustic pressure of 2.9 kPa was generated at an elevation of around 14 cm, which decreases as the elevation increases or decreases. This is clearly justified by the fact that as the elevation increases (beyond 14 cm in this case), the focal point size increases which results in a decreased average pressure (further attenuation was also experienced but neglected here). On the other hand, as the elevation decreased below the 14 cm height, some transducers

were not able to contribute to the formation of the focal point (due to limited directivity). Therefore, it would be best to have the center of the device workspace for one tile at the 14 cm elevation since this will produce maximized tactile stimulation.

C. 2D TACTILE STIMULATION

For the 2D tactile stimulation, we considered two 2D shapes: a straight line and a circle. The scan volume was adjusted with the following configuration: 100×100 mm, step size of 2 mm (giving a total of 2500 measurements for a single slice of xy-plane). The robotic arm performed 10 slices of measurements along the vertical axis that are centered at the elevation where the 2D shape was generated. We report only the acoustic pressure distribution at the desirable elevation. Note that 200 focal points were used to generate the 2D objects (straight line and circle). The rendering frequency is set to 10 Hz.

FIGURE 18. Theoretical circle stimulated at 12 cm elevation (scale in m).
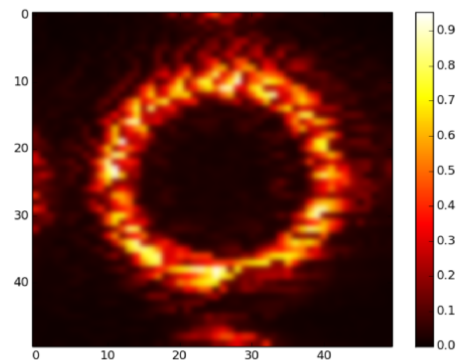
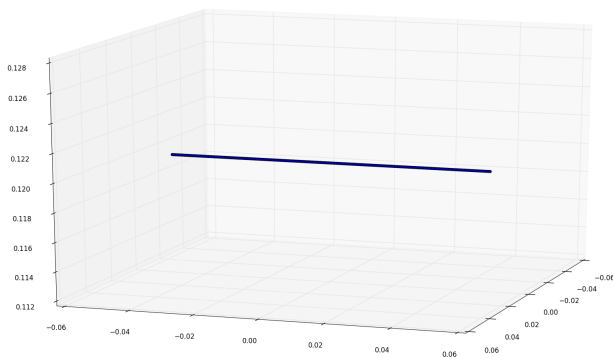FIGURE 19. Experimental circle stimulated at 12 cm elevation (scale in mm).

FIGURE 16. Theoretical straight line stimulated at 12 cm elevation (m).
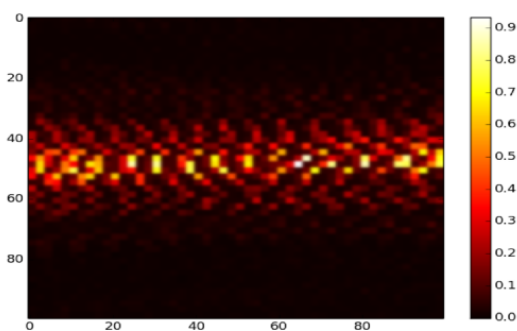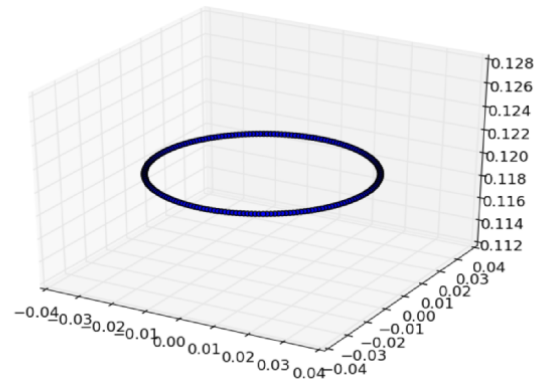

FIGURE 17. Experimental straight line stimulated at 12 cm elevation (mm).

Figure 16 and Figure 18 show the point cloud distribution of focal points for the straight line and circle shapes, respectively, at 12 cm elevation. Figure 17 and Figure 19 show the spatial distribution of the acoustic pressure for the two 2D shapes (straight line and circle respectively) that are generated from the ultrasound array surface. The amplitude is normalized with a maximum force of 2.9 kPa. Figure 17 shows a clear straight line centered along the y-axis and

spread along 100 mm. Similarly, Figure 19 demonstrates clearly a circle with a diameter of around 70mm.

D. 3D TACTILE STIMULATION

For the 3D tactile stimulation, we considered the display of the upper hemisphere whose center is located at an elevation of 14 cm, with a radius of 50 mm, using 200 focal points. The rendering frequency is 7 Hz. The scan volume was adjusted with the following configuration: 100mm by 100 mm, step size of 2 mm (giving a total of 2500 measurements for a single slice of a horizontal plane). The robotic arm performed 20 slices of measurements along the vertical axis that started from height 14 cm up to 24 cm, with a step size of 5 mm between slices.

Figure 20 shows the theoretical point cloud for the hemisphere object. Figure 21 shows the spatial distribution of the acoustic pressure for the hemisphere object that is centered at an elevation of 14 cm. Note that in Figure 21, only pressures above 2 kPa are displayed to clearly demonstrate the formation of a hemisphere by the formation of 200 focal points.

E. DISCUSSION

The experimental analysis has clearly demonstrated the ability of th Haptogram system to generate perceivable tactile
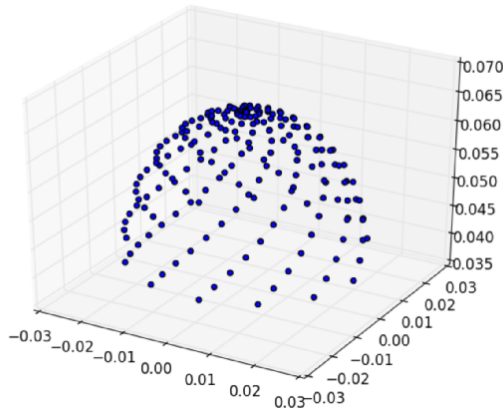
FIGURE 20. Theoretical hemisphere centered at 14 cm elevation (scale in m).
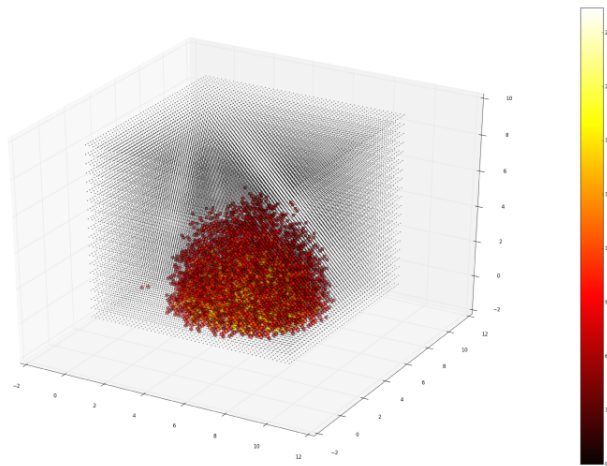

FIGURE 21. Experimental hemisphere centered at 14 cm elevation (1 division on the figure corresponds to 1 cm).

objects (single point, 2D shapes and 3D shapes). One tile of the Haptogram display was able to generate an average force of 2.65 kPa (standard deviation of 0.2 kPa) for the 200 focal points that make up the 3D shape, over an elevation range of 8 cm to 18 cm. The rendering frequency for the 3D shape is 7 Hz.

The Haptogram system has several advantages over existing ultrasonic tactile display approaches. First of all, since it is point- cloud based, high resolution of 3D tactile objects can easily be rendered. Second, high rendering frequency can be achieved so that the Haptogram system is capable of displaying high fidelity tactile stimulation. The Haptogram system provides users the utility to trade tactile stimulation intensity (via rendering frequency) and resolution of tactile display (via the number of displayed focal points). There is a tradeoff between rendering frequency and number of focal point to guarantee maximum acoustic pressure.

An audible sound is heard when the Haptogram system is turned on. Headphones for ear protection can be used to prevent hearing it. There are two sources of the audible sound.

One is the envelope of the ultrasound. If 500 Hz modulation is used, the 500 Hz audible sound is produced due to the non-linearity of air, which is a phenomenon utilized in a directive loudspeaker [24]. The other cause would be the discontinuity of the phases of the driving signals when the position of the focal point is changed. We believe that the former source is the dominant one.

Finally, there might have been few sources of errors while taking measurements via the robotic arm. For instance, the surface of the ultrasound array and the scanning surface of the robotic arm may not be perfectly parallel. This implies that there might be some errors measuring forces at a particular horizontal slices due to skewed measurement. Another potential source of errors is due to additional ultrasonic reflections as the robotic arm comes closer to the surface of the array of transducers.

V. USABILITY STUDY
The purpose of this study is to investigate how well users can perceive animated 2D shapes displayed by the Haptogram system. Although 3D shapes can be presented, we decided to limit this study to 2D objects. We plan to investigate the quality of user experience for 3D objects in future research. Four 2D shapes are considered: circle, triangle, line and a plus sing (shown in Figure 22).
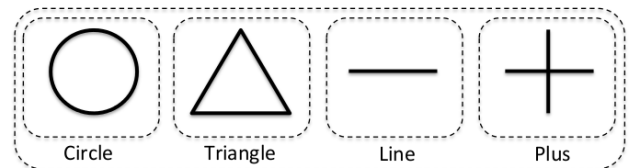

FIGURE 22. The four 2D shapes used for the experimental study.

A. EXPERIMENTAL DESIGN
The shapes were randomly selected and displayed in a square of 10 cm by 10 cm workspace with a precision of 1 mm. Users were asked to feel the tactile stimulation through their palm. The users were also given noise cancellation headphones to eliminate acoustic noise generated by the system or any other auditory source that may distract the user from recognizing the tactile shape. A snapshot of a user performing the experiment is shown in Figure 23.

The following configurations were used for tactile stimulation: the rendering frequency is set to 10 Hz while the number of focal points is set to 200. The shapes stimuli were displayed in a random order to reduce the bias and ordering effects as much as possible. For each trial, we measured two parameters: the recognition rate and the recognition time. We define the recognition rate as the ratio of accurately identifying a displayed shape over the total number of trials. The recognition time is the average time it took the user to recognize a particular shape correctly. The experiment is divided into two blocks of 12 trials for each

block, giving participants time to rest from a trial to the next.

B. TASK

Our task required users to recognize one of the four 2D shapes by holding their hands on top of the Haptogram display. The elevation of tactile stimulation is fixed since the user is asked to rest his/her palm on a stand tuned at 13 cm elevation (the elevation at which the shapes are generated). No audio-visual cues about the displayed 2D shapes were given to the subjects. Each trial started when the participant hit the return button of the keyboard in front of them. Once a trial starts, the participant should feel tactile shapes on his/her palm and respond as fast and accurate as possible. The participant responds by keying a corresponding number (1 for circle, 2 for plus sign, 3 for line, and 4 for triangle). Each shape is displayed continuously for a maximum of 30 seconds. If the user fails to give a response within the 30 seconds, then the trial is cancelled. As soon as the user gives a response, the response time is recorder along with whether the selection was correct or not. Next, the user is given some time to rest before proceeding to the next trial.
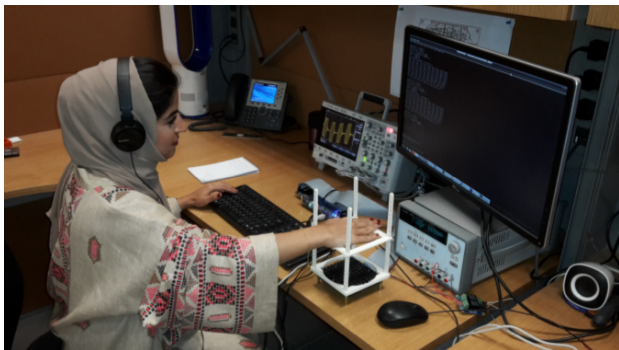

FIGURE 23. A user performing the experiment.

C. APPARATUS

A one-tile Haptogram prototype (10×10 transducers) is used in this experiment. The experiment software was running on a desktop PC equipped with an Dual Six CoreXEON E5-2630, 2.3G Hz processor and 32 GB RAM. A hand-resting stand was designed specifically for this experiment (shown in Figure 23). Active noise-cancelling headphones were used to cancel out the auditory noise.

D. PARTICIPANTS

Fifteen (15) adult subjects were participated in the experiment; 8 male, 7 female, average age of 26 years (standard deviation was 6.60 years). By self-reporting, none of the subjects had any deficiency in their ability to touch. Users were allowed a training session for as much as they desire to familiarize themselves with the system and the stimuli before completing the experiment. In total, we collected 360 trials (15 participants $\times$ 2 sessions $\times$ 12 trials per session).

E. RESULTS

The overall recognition rate for all subjects was well above the chance level (average of 59.44%, standard deviation of 12.75%). The overall recognition time has an average of 13.87 seconds and a standard deviation of 3.92 seconds.

Looking at the recognition rate for each shape, we found that the plus sign shape was the easiest to recognize while the line shape was the most difficult to recognize. This could be because the line shape is easier to confuse with the circle and/or triangle shapes. The average recognition rate for all the shapes, along with the standard deviations, are shown in Figure 24. It is also observed that one participant never got the triangle shape.
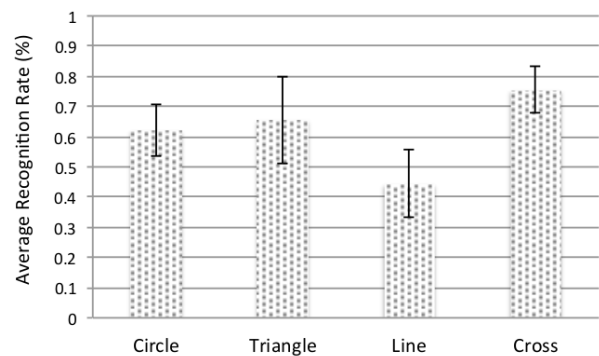

FIGURE 24. Average and standard deviation for the recognition rate of the four 2D shapes.
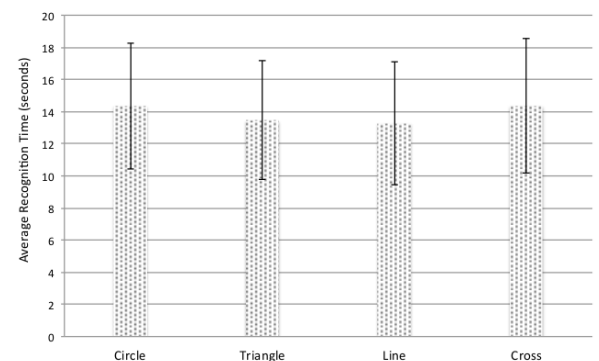

FIGURE 25. Average and standard deviation for the recognition time of the four shapes.

As for the recognition time, results show that the plus sign shape has the largest recognition time compared to other shapes while the line shape has the lowest recognition time (Figure 25). However, the differences are not that significant to derive definite conclusions about the recognition speed for each shape; more or less all shapes have similar recognition times.

Finally, in an effort to recognize what shapes were the most confusing, we analyzed the data to find errors across combinations of shapes. Table 1 shows the results. For instance, the 14.45% is the percentage of confusing the triangle shape as a circle, and so on. It seems that the line shape is mostly

TABLE 1. Confusion matrix across the four shapes.

	Circle	Triangle	Line	Plus sign
Circle	**62.23%**	6.67%	26.67%	4.45%
Triangle	14.45%	**65.56%**	12.23%	7.78%
Line	51.12%	2.23%	**44.45%**	2.23%
Plus sign	6.67%	10.00%	7.78%	**75.56%**

confused with circle (51.12% of the times line was confused and recognized as circle). The circle is also highly confused with the line (26.67%). The most clearly perceived shape was the plus sign; it has around 75% recognition rate, and is been confused the least among the four shapes.

Even thought it would be hard to derive statistically valid conclusions, we also observed a considerable improvement in performance from session to session; there has been a 14% improvement in the recognition rate and a 12% decrease in the recognition time. This clearly shows that users have quickly learned how to use the device and effectively perceive 2D shapes.

VI. CONCLUSION

In this paper, we presented a system called Haptogram that is capable of displaying 3D tactile objects via point-cloud representation. The current prototype has one tile of two-dimensional array of ultrasound transducers (10×10 transducers). A thorough performance study is presented to characterize the Haptogram system as a haptic display for various tactile shapes (single point, 2D shapes, and 3D shapes). As a result, it is confirmed that: 1) humans can feel a localized focal point clearly (average force generated is 2.9 kPa which is well above what human skin can perceive [25]) and 2) the Haptogram system is capable of producing a high rendering frequency and thus is capable of generating high fidelity tactile display (1.62 kHz in the current implementation).

As for future work, first of all we plan to expand the system workspace to four tiles. We are currently in the development phase of these four tiles. We will investigate the effect of increasing the number of tiles on the quality parameters for the Haptogram display. The performance evaluation with more complex 3D objects will be studied with four tiles of tactile display. Another important step will be to conduct a usability study to evaluate the quality of user experience while using the Haptogram system. Finally, we plan to combine the Haptogram tactile display with a hologram display so that an immersive multimodal system can be created and tested.

REFERENCES

[1] S. Comai and D. Mazza, "Integrating haptics in Web interfaces: State of the art and open issues," *IEEE Internet Comput.*, vol. 16, no. 5, pp. 83–87, Sep. 2012.

[2] D. Dalecki, S. Z. Child, C. H. Raeman, and E. L. Carstensen, "Tactile perception of ultrasound," *J. Acoust. Soc. Amer.*, vol. 97, no. 5, pp. 3165–3170, 1995.

[3] R. Sodhi, I. Poupyrev, M. Glisson, and A. Israr, "Aireal: Interactive tactile experiences in free air," *ACM Trans. Graph.*, vol. 32, no. 4, Jul. 2013, Art. no. 134.

[4] Y. Suzuki and M. Kobayashi, "Air jet driven force feedback in virtual reality," *IEEE Trans. Comput. Graph. Appl.*, vol. 25, no. 1, pp. 44–47, Jan./Feb. 2005.

[5] H. Lee *et al.*, "Mid-air tactile stimulation using laser-induced thermoelastic effects: The first study for indirect radiation," in *Proc. IEEE World Haptics Conf. (WHC)*, Jun. 2015, pp. 374–380.

[6] E. S. Ebbini and C. A. Cain, "Multiple-focus ultrasound phased-array pattern synthesis: Optimal driving-signal distributions for hyperthermia," *IEEE Trans. Ultrason., Ferroelectr., Freq. Control*, vol. 36, no. 5, pp. 540–548, Sep. 1989.

[7] T. Hasegawa, T. Kido, T. Iizuka, and C. Matsuoka, "A general theory of rayleigh and langevin radiation pressures," *J. Acoust. Soc. Jpn.*, vol. 21, no. 3, pp. 145–152, 2000.

[8] T. Iwamoto and H. Shinoda, "Two-dimensional scanning tactile display using ultrasound radiation pressure," in *Proc. 14th Symp. Haptics Inter. Virtual Environ. Teleoper. Syst.*, Mar. 2006, pp. 57–61.

[9] T. Iwamoto, M. Tatezono, and H. Shinoda, *Non-Contact Method for Producing Tactile Sensation Using Airborne Ultrasound* (Lecture Notes in Computer Science), vol. 5024 LNCS. Tokyo, Japan: Univ. Tokyo, 2008.

[10] T. Hoshi, M. Takahashi, T. Iwamoto, and H. Shinoda, "Noncontact tactile display based on radiation pressure of airborne ultrasound," *IEEE Trans. Haptics*, vol. 3, no. 3, pp. 155–165, Jul./Sep. 2010.

[11] K. Hasegawa and H. Shinoda, "Aerial display of vibrotactile sensation with high spatial-temporal resolution using large-aperture airborne ultrasound phased array," in *Proc. World Haptics Conf. (WHC)*, Univ. Tokyo, Japan, 2013, pp. 31–36.

[12] K. Yoshino and H. Shinoda, "Visio-acoustic screen for contactless touch interface with tactile sensation," in *Proc. World Haptics Conf. (WHC)*, Apr. 2013, pp. 419–423.

[13] K. Yoshino and H. Shinoda, "Contactless touch interface supporting blind touch interaction by aerial tactile stimulation," in *Proc. IEEE Haptics Symp. (HAPTICS)*, Feb. 2014, pp. 347–350.

[14] S. Inoue, Y. Makino, and H. Shinoda, "Active touch perception produced by airborne ultrasonic haptic hologram," in *Proc. IEEE World Haptics Conf. (WHC)*, Jun. 2015, pp. 362–367.

[15] L. R. Gavrilov, "The possibility of generating focal regions of complex configurations in application to the problems of stimulation of human receptor structures by focused ultrasound," *Acoust. Phys.*, vol. 54, no. 2, pp. 269–278, Mar. 2008.

[16] T. Carter, S. Seah, B. Long, S. Subramanian, and B. Drinkwater, "Ultrahaptics: Multi-point mid-air haptic feedback for touch surfaces," in *Proc. 26th Annu. ACM Symp. User Interface Softw. Technol. (UIST)*, 2013, pp. 505–514.

[17] B. Long, S. Seah, T. Carter, and S. Subramanian, "Rendering volumetric haptic shapes in mid-air using ultrasound," *ACM Trans. Graph.*, vol. 33, no. 6, Nov. 2014, Art. no. 181.

[18] S. Inoue, Y. Makino, and H. Shinoda, "Producing airborne ultrasonic 3d tactile image by time reversal field rendering," in *Proc. SICE Annu. Conf.*, Univ. Tokyo, Japan, Sep. 2014, pp. 1360–1365.

[19] T. Hoshi, H. Shinoda, and T. Iwamoto, "Non-contact tactile sensation synthesized by ultrasound transducers," in *Proc. 3rd Joint Eur. Haptics Conf. Symp. Haptic Interfaces Virtual Environ. Teleoper. Syst. World Haptics*, Mar. 2009, pp. 256–260.

[20] S.-E. Måsøy *et al.*, "Nonlinear propagation acoustics of dual-frequency wide-band excitation pulses in a focused ultrasound system," *J. Acoust. Soc. Amer.*, vol. 128, no. 5, pp. 2695–2703, 2010.

[21] T. Hoshi, "Development of aerial-input and aerial-tactile-feedback system," in *Proc. IEEE World Haptics Conf. (WHC)*, Jun. 2011, pp. 569–573.

[22] L. Azar, Y. Shi, and S.-C. Wooh, "Beam focusing behavior of linear phased arrays," *NDT E Int.*, vol. 33, no. 3, pp. 189–198, Apr. 2000.

[23] E. Moros, *Physics of Thermal Therapy: Fundamentals and Clinical Applications*. Boca Raton, FL , USA: CRC Press, 2012, ch. 6, p. 96.

[24] M. Yoneyama, J.-I. Fujimoto, Y. Kawamo, and S. Sasabe, "The audio spotlight: An application of nonlinear interaction of sound waves to a new type of loudspeaker design," *J. Acoust. Soc. Amer.*, vol. 73, no. 5, p. 1532, 1983.

[25] L. Skedung, M. Rutland, M. Arvidsson, B. Berglund, J. Chung, and C. Stafford, "Feeling small: Exploring the tactile perception limits," *Sci. Rep.*, vol. 3, p. 2617, Sep. 2013.

GEORGIOS KORRES (M'16) was born and raised in Athens, Greece. He received the B.Sc. degree in applied mathematics from the School of Science and Engineering, University of Crete. He was involved for several years with the development of educational software and hardware regarding educational robotics. In the last three years, he has also dealt with industrial automation (mainly in the field of recycling industry). His research interests focus on development of new sensors and actuators as well as the use of these in human computer interaction.

MOHAMAD EID (SM'06) received the Ph.D. degree in electrical and computer engineering from the University of Ottawa, Canada, in 2010. He is currently an Assistant Professor of electrical engineering at New York University Abu Dhabi. He was previously a Teaching and Research Associate at the University of Ottawa from 2008 to 2012. He is the co-author of the book *Haptics Technologies: Bringing Touch to Multimedia* (Springers, 2011), the Co-Chair of the 3rd International IEEE Workshop on Multimedia Services and Technologies for E-health, and the Technical Chair of the Haptic-Audio-Visual Environment and Gaming workshop in 2013. He is a recipient of the best paper award of the DS-RT 2008 Conference and the prestigious ACM Multimedia 2009 Grand Challenge Most Entertaining Award for HugMe: Synchronous Haptic Teleconferencing System. He has over 75 conference and journal papers and five patents. His academic interests include multimedia haptics, affective haptics, and tangible human computer interaction for assistive living.

• • •